Research Paper

Volume : 4 | Issue : 6 | June 2015 • ISSN No 2277 - 8179

The Effect of Storm Surge and Tidal Currents to Sediment Transport in the North Ariake Sea, Japan

International Journal of Scientific Research

Engineering

KEYWORDS : North Ariake Sea, Sediment Transport and Tidal current, Storm Surge

Tommy Jansen — Department of Civil Engineering and Architecture, Saga University Honjomachi, Saga , Japan

Koichiro Ohgushi — Civil Engineering Department, Sam Ratulangi University Kampus Unsrat Bahu, Manado, Indonesia

ABSTRACT

The Ariake Sea in Japan is a typical semi-enclosed shallow sea being rich in fishery products. The amount of fishery products decrease in recent years. The prediction of tidal flow, wind effect and suspended sediment transport are important. As analytical tools, MIKE3 Hydrodynamic and Mud Transport Model are used. The simulated tidal current are based on the observation at Nagasaki and Typhoon Songda 200418 from 28 August to 7 September 2004. The highest Suspended Sediment Concentration appeared near the river mouth caused by flooding and behavior of Suspended Sediment Concentration from north to south at spring and neap tides. Storm Surge effected the erosion taking place at most areas in north Ariake Sea and influenced the most to suspended sediment during strong wind period.

INTRODUCTION

Ariake sea is a typical semi-enclosed shallow sea being rich in fishery products.

It supports the local economy through fishing and the cultivating grounds of fish and shellfish. The amount of fishery products have decreased in recent years. The reason is clear that the seabed deposit has been deteriorated. While the sea is being degraded, water quality is suffering and soil particles of tidal flats is decreasing. Considering that the decline in the shellfish production was the most serious signal of the environmental degradation of Ariake bay (H.Nakata et al.,2010). For this reason, the prediction of tidal flow, wind effect and suspended sediment transport are important in coastal related areas. Kyushu island is often passed by typhoons. In this island there is Ariake Sea characterized by a macro tidal range (3-6m) because of the largest tidal range in Japan (Kato and Seguchi,2001 ; Hiramatsu et al.,2005 ; Tsusumi,2006). The influence of typhoon on the basin strongly depends on its tracks and wind speed. Typhoon Songda space200418 is the one of the most serious typhoon which track in the area.

The purpose of the research regarding to condition of sediment concentration may have on the aquatic environment of North Ariake Sea caused by tidal current, storm surge and the relative contribution in support of ecosystem restoration.

II. STUDY AREAS

The North Ariake Sea locates in the west of Kyushu Japan. The total area of this sea is approximately 1,700km^2. Tidal flats cover 18,840ha in this part, receiving flow of some rivers. Among them Chikugo river is the largest river in which the estuary connects to the North Ariake bay.

Figure 1. Study Area

III. METHODOLOGY

III.1 Computational Tools

As the computational tools the MIKE3 Flow Model Flexible Mesh (MIKE3 FM) HD Hydrodynamic and MT Mud Sediment Transport by DHI (Denmark Hydraulic Institute) are used.

The main characteristic of this tools are :

Dimension work is 3D, integral method is Eulerian, coordinate vector system is Cartesian, the cell element used prisms-triangular extrusion, method of generation mesh used triangulation-Delaunay, the finite approximation for transport equation used FVM, finite approximation for hydrodynamic equations used FEM/FVM.

III.2 Calculation Method

The model is base on the solution of the three dimensional incompressible Reynolds averaged Navier-Stokes equations, subject to the assumption of Boussinesq and of hydrostatic pressure.

The equation of continuity :

$$\frac{\partial u}{\partial x}+\frac{\partial v}{\partial y}+\frac{\partial w}{\partial z}=S \qquad (1)$$

The momentum equations:

The two horizontal momentum equations for the x and y component, respectively :

$$\frac{\partial u}{\partial t}+\frac{\partial u^2}{\partial x}+\frac{\partial vu}{\partial y}+\frac{\partial wu}{\partial z}=fv-g\frac{\partial \eta}{\partial x}-\frac{1}{\rho_0}\frac{\partial p_a}{\partial x}-\frac{g}{\rho_0}\int_z^\eta\frac{\partial \rho}{\partial x}dz-\frac{1}{\rho_0 h}\left(\frac{\partial S_{xx}}{\partial x}+\frac{\partial S_{xy}}{\partial y}\right)+Fu+\frac{\partial}{\partial z}\left(v_t\frac{\partial u}{\partial z}\right)+u_sS \qquad (2)$$

$$\frac{\partial v}{\partial t}+\frac{\partial v^2}{\partial y}+\frac{\partial uv}{\partial x}+\frac{\partial wv}{\partial z}=-fu-g\frac{\partial \eta}{\partial y}-\frac{1}{\rho_0}\frac{\partial p_a}{\partial y}-\frac{g}{\rho_0}\int_z^\eta\frac{\partial \rho}{\partial y}dz-\frac{1}{\rho_0 h}\left(\frac{\partial S_{yx}}{\partial x}+\frac{\partial S_{yy}}{\partial y}\right)+Fv+\frac{\partial}{\partial z}\left(v_t\frac{\partial v}{\partial z}\right)+v_sS \qquad (3)$$

Where t is the time, x,y and z are the Cartesian co-ordinates; ηis the surface elevation; d is the still water depth; h=η+d is the total water depth; u,v and w are the velocity components in x,y,z direction; f=2ΩSinφ is the Coriolis parameter (Ωis the angular rate

of revolution and φis geographic latitude); g is the gravitational acceleration; ρis the density of water; S_{xx},S_{yx},S_{xy} and S_{yy} are components of the radiation stress tensor; v_t is the vertical turbulent viscosity; p_a is the atmospheric pressure; ρ_0 is the reference density of water; S is the magnitude of discharge due to point sources and (u_s,v_s) is the velocity by which the water is discharged into the ambient water.

The horizontal stress terms are described using a gradient-stress relation, which is simplified to:

$$Fu = \frac{\partial}{\partial x}\left(2A\frac{\partial u}{\partial x}\right) + \frac{\partial}{\partial y}\left(A\left(\frac{\partial u}{\partial y} + \frac{\partial v}{\partial x}\right)\right) \quad (4)$$

$$Fv = \frac{\partial}{\partial x}\left(A\left(\frac{\partial u}{\partial y} + \frac{\partial v}{\partial x}\right)\right) + \frac{\partial}{\partial y}\left(2A\frac{\partial v}{\partial y}\right) \quad (5)$$

where A is the horizontal eddy viscosity.

Transport equation for salt:

$$\frac{\partial s}{\partial t} + \frac{\partial us}{\partial x} + \frac{\partial vs}{\partial y} + \frac{\partial ws}{\partial z} = F_s + \frac{\partial}{\partial z}\left(D_v\frac{\partial s}{\partial z}\right) + s_s S \quad (6)$$

$$F_s = \left[\frac{\partial}{\partial x}\left(D_h\frac{\partial s}{\partial x}\right) + \frac{\partial}{\partial y}\left(D_h\frac{\partial s}{\partial y}\right)\right](s) \quad (7)$$

The diffusion coefficients can be related to the eddy viscosity:

$$D_h = \frac{A}{\sigma_T} \qquad D_v = \frac{v_t}{\sigma_T} \qquad (8)$$

Where D_v is vertical turbulent (eddy) diffusion coefficient, s_s is salinity of the source, F is horizontal diffusion terms, D_h is horizontal diffusion coefficient, σ_T is Prandtl number.

The transport of the mud:

The transport of the mud is generally described by the equation (e.g.Teisson, 1991):

$$\frac{\partial c}{\partial t} + \frac{\partial uc}{\partial x} + \frac{\partial vc}{\partial y} + \frac{\partial wc}{\partial z} - \frac{\partial w_s c}{\partial z} = \frac{\partial}{\partial x}\left(\frac{v_{Tx}}{\sigma_{Tx}}\frac{\partial c}{\partial x}\right) + \frac{\partial}{\partial y}\left(\frac{v_{Ty}}{\sigma_{Ty}}\frac{\partial c}{\partial y}\right) + \frac{\partial}{\partial z}\left(\frac{v_{Tz}}{\sigma_{Tz}}\frac{\partial c}{\partial z}\right) + S \quad (9)$$

Where t is the time, x,y and z are Cartesian co-ordinate, u,v and w are flow velocity component, c is mass concentration, w_s is fall velocity, σ_{Tx} is turbulent Schmidt number, v_{Tx} is anisotropic eddy viscosity, S is source term.

Settling velocity:

The settling velocity of the suspended sediment may be specified as a constant value. Flocculation is described as a relationship with the suspended sediment concentration (Burt,1986). Hindered settling can be applied if the suspended sediment concentration exceeds a certain level. To distinguish between three different settling regimes, two boundary are defines, c_{floc} and $c_{hindered}$, being the concentrations where flocculation and hindered settling begins, respectively.

Constant settling velocity:

The flocculation may be negligible while suspended sediment concentration is below a certain value, and constant settling velocity can be applied:

$$w_s = k \qquad c \prec c_{floc} \qquad (10)$$

Where w_s is the settling velocity and k is the constant.

Flocculation:

The sediment will begin to flocculate after reaching c_{floc}. The relationship between settling velocity and sediment density (Burt,1986):

$$w_s = k\,x\left(\frac{c}{\rho_{sediment}}\right)^{\gamma} \qquad c_{floc} \succ c \succ c_{hindered} \quad (11)$$

Where k is a constant, $\rho_{sediment}$ is the sediment density, γ is a coefficient termed settling index.

Hindered settling:

The settling column of flocs begin to interfere after a relatively high sediment concentration ($c_{hindered}$) is reached and hereby reducing the settling velocity.

Deposition:

The relationship within the deposition as (Krone,1962)

$$S_D = w_s c_b p_d \qquad (12)$$

where w_s is the settling velocity of the suspended sediment (ms^{-1}), c_b is the suspended sediment near the bed, p_d is the probability of deposition.

$$p_d = 1 - \frac{\tau_b}{\tau_{cd}} \qquad (13)$$

In the three-dimensional model, c_b is simply equal to the sediment concentration in the water cell just above the sediment bed.

Erosion :

Erosion for hard-bed:

The erosion rate for a consolidated bed can be written as (Partheniades,1965):

$$S_E = E\left(\frac{\tau_b}{\tau_{ce}} - 1\right)^n \qquad \tau_b \succ \tau_c \qquad (14)$$

Where E is the erodibility (kg m^{-2} s^{-1}), n is the power of erosion,τ_b is the bed shear stress (N m^{-2}) and τ_{ce} is the critical shear stress for erosion (N m^{-2}). S_E is the erosion rate (kg m^{-2} s^{-1}).

Erosion for soft-bed:

The erosion rate of the partly consolidated bed can be written as (Parchure and Mehta,1985):

$$S_E = E\left(e^{\alpha\sqrt{(\tau_b - \tau_c)}}\right) \qquad \tau_b \succ \tau_c \qquad (15)$$

Where α is the empirical constant for erosion.

Model setting and data :

In the model setting, a finite difference grid was developed as the model domain with the size of the triangular mesh option which each element maximum area is 1,000,000 m^2. The vertical direction z is divided into 10 layers. The horizontal grid mesh contains 256,250 element with 152,196 nodes. The model was calibrated with using observed data between August and September, 2004 (reference 2 and 9). During calibration the parameter of hydrodynamic and sediment characteristics of the sea were adjusted until a satisfactory correspondence between the model results and observed field data was obtained.

The critical shear stress τ_{ce} = 0 to 0.4 Pa, was used for start the sediment resuspension value. The coefficient erosion (E) is a factor used to control the overall level of the erosion (Eqs.14,15).

The calibrated rate of erosion E=0.00001 kg m^{-2} s^{-1}. The empirical constant for erosion α=1, the power of erosion n=1. Bed roughness, z_0= 0.001 to 0.005 m.

The data needed as input are: bathymetric data obtained from the Ariake Sea Project of Saga University in the form of water depth in the Ariake sea and other areas in the southern of Kyushu Island in longitude 129^0 - 130^0 and latitude 32^0 - 33^0. The topographic data are obtained from 50 m DEM of Japan supplied by Geospatial Information Authority of Japan. The discharge data of Chikugo, Yabe, Rokkaku and Kase river are obtained from Japan Water Information System. The high intensity of rainfall effect to the river can be shown in the data as high discharge (flooding). The tidal current considered is Nagasaki Tide, the data are obtained from Japan Oceanographic Data Center. The Storm Surge is Typhoon Songda200418 from 28 August to 7 September 2004 in the form of wind speed and direction, obtained from Japan Meteorology Agency.

III.3.Initial Condition and Boundary Condition:

The hydrodynamic initial condition is a form of surface water level data on 28 August, 00:00:00, 2004 which is interpolated by using data from several station Nagasaki, Kuchinotsu, Misumi and Oura.

The salinity initial condition is a data file containing initial salinity value (PSU) where the data is varying in domain. The data value were preset in the range 30 to 32 PSU , for the temperature is taken as constant value.

The mud transport initial condition were preset as suspended sediment concentration constant value in domain, were preset in the range 0 to 0.024 kg m^{-3}.

The hydrodynamic boundary condition is a form of time series discharge of Chikugo, Yabe , Rokkaku and Kase river from 28 August, 00:00:00 to 7 September,23:00:00, 2004 and Nagasaki Tide as boundary condition at open sea of Ariake.

The salinity boundary condition is specified value as varying in time and along boundary at open sea of Ariake, were preset in the range 31 to 33 PSU . For the rivers, salinity value were preset 0 PSU with assumption that at the start of simulation the water from river still be as fresh water.

The mud transport boundary condition for rivers and the open sea were preset in the range 0.001 to 0.02 kg m^{-3}.

IV. RESULT AND DISCUSSION

IV.1 Model Calibration

Calibration of the model for water surface level at Nagasaki and Kuchinotsu, are shown in Fig.2 and 3. Calibration of the model for salinity and suspended sediment can be shown in Fig.4 and 5. Fig. 2 and 3 show the good result between simulation and measurement of Kuchinotsu and Nagasaki water levels. Fig.4 shows the good result between simulation and measurement in the area where the range of salinity is from 26 to 29PSU (reference 9). Fig.5 shows the good result of simulation and measurement in Sta S6 near the Chikugo river estuary which SSC measurement data being from 0.03 to 0.04 kg/m^3 (reference 2).

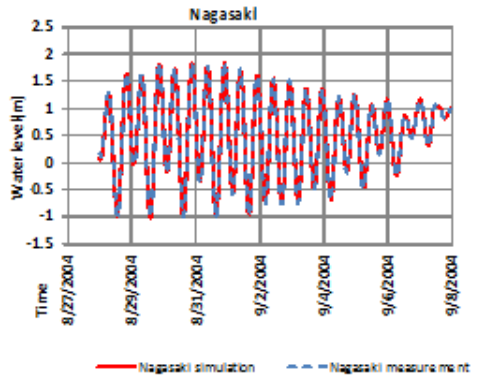

Figure 2. Calibration of Water level at Nagasaki

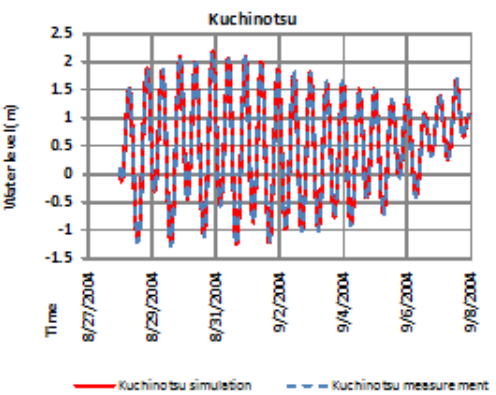

Figure 3. Calibration of Water level at Kuchinotsu

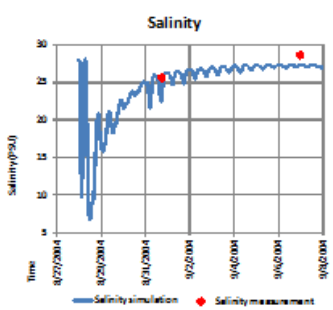

Figure 4. Calibration of salinity

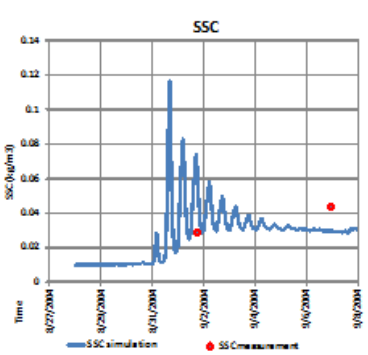

Figure 5. Calibration of SSC

IV.2 Simulation Result and Discussions

Fig.6 indicates that during flooding the highest SSC takes place near the river mouth to seaward and by tidal current from south to the north at spring tide. The result well reflects the characteristics of SSC distribution in the mouth of river that includes tidal flats, where the concentration are higher than those not only at upstream part but the offshore parts as well. It moves concurrent by flooding flow. Concentration of the flat part are higher than those other place because sediments on the flats are more abundant and easier to be stirred up. The interface of saline water and fresh water (Fig. 7) can be clearly seen around the river mouth. Viewing the vertical distribution of salinity, the low salinity water moves offshore at the surface while the bottom saline water conversely moves more to upstream.

A graph trend of bed thickness tends to decrease (graph lines below 0.0m) at south part of North Ariake Sea (Fig.8,9).The maximum decrease of bed thickness in this graph about 0.1 m below the bed initial surface. This indicates that erosion average took place in this part. Fig.10 shows tendency of the bed thickness increasing (graph lines above 0.0m) in north part effected by tidal current. The maximum increasing of bed thickness in this graph was very small. This indicates that deposition average took place in this part. Fig.11 shows tendency of the bed thickness decreasing by storm surge (graph lines below 0.0m). The concentration of the graph lines are near the date of 31 August 2004, because the peak of strong wind took place near this date . The effect of wind by Songda to Saga denotes that erosion took place at almost of the all points in the basin of north part Ariake sea (Fig.11), This indicates that storm surge generated by typhoon stirs up large quantity of sediment resulting the tidal flats` erosion.

At stratification`s checking point IP12 (right side line through Chikugo river) for example (Fig.12) and in Fig.13 show that current velocity at water surface higher than bottom by taking red line graph (TS236) with assumption that there is a delay between peak of velocity and peak of water level.

This condition is same as stratification`s

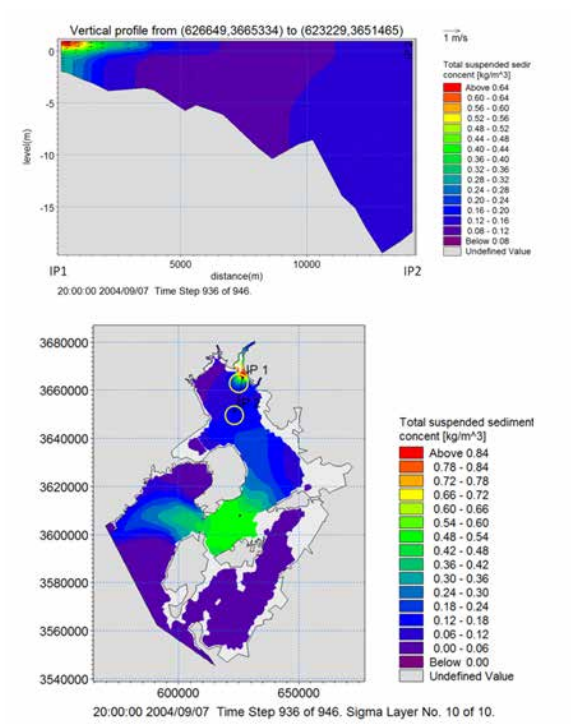

Figure 6. SSC vertical profile along IP1-IP2 line with SSC horizontal distribution in Ariake Sea

checking point at the left side line through Kase River. The SSC in this location can be shown in Fig.14. The values of current velocity and SSC of IP1 to IP13 are denoted in Table 1 and 2. In Table 2, it is apparent that values of SSC are higher in near the mouth of river than at seaward.

The highest value of SSC was transported by flooding from upstream to the mouth of river in Chikugo River and the lower value of SSC was transported by tidal current from south to the north at spring tide and conversely at the neap tide.

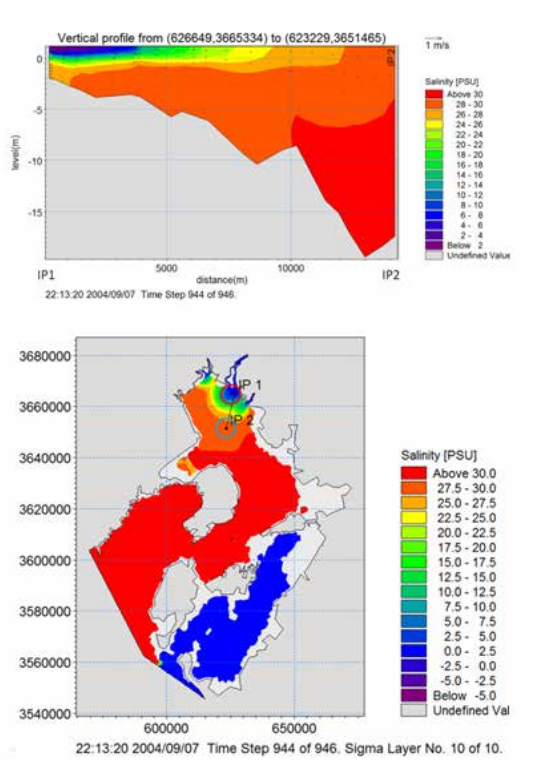

Figure 7.Salinity vertical profile with salinity horizontal distribution in the Ariake Sea

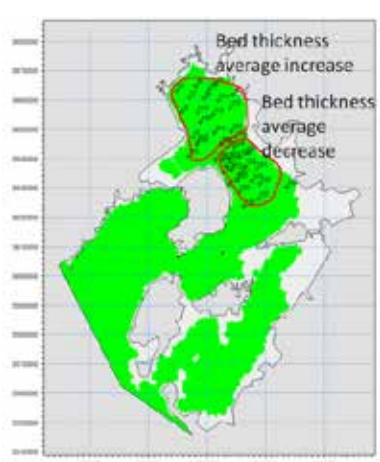

Figure 8. Bed thickness increase and decrease trend location in North Ariake Sea effected by tide.

Figure 9. Bed thickness trend.

Figure 10. Average bed thickness

Figure 11. Average bed thickness trend, effect of the

Volume : 4 | Issue : 6 | June 2015 • ISSN No 2277 - 8179

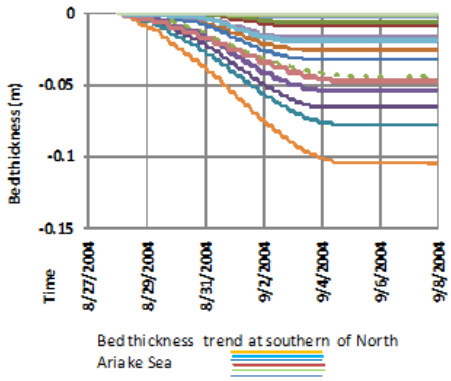

Figure 9. Bed thickness trend.

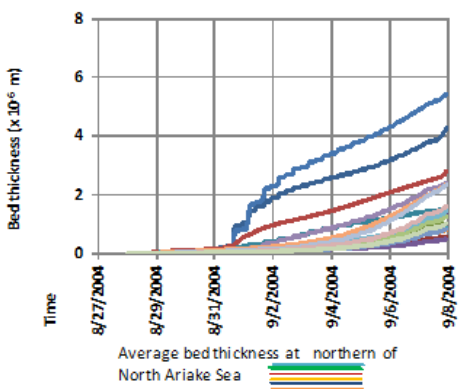

Figure 10. Average bed thickness

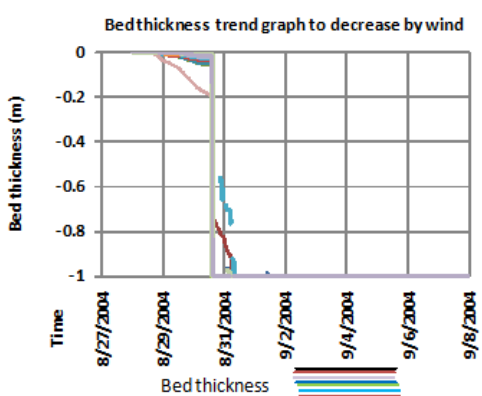

wind for decrease of the bed thickness..

In Table 1 it is shown that the current velocity effected by the flooding tide is gradually influenced through IP1 until IP5 from strong to weak influence of current speed. In the case of tide and wind taking place concurrent, SSC will be higher at strong wind time and after this time, the value of SSC decreases and almost the same to the tide effect. It can be shown in Fig.15 to Fig. 17 at surface layer and bottom layer, which the redt color is effected by tide and blue color is effected by tide-wind concurrent taken place.

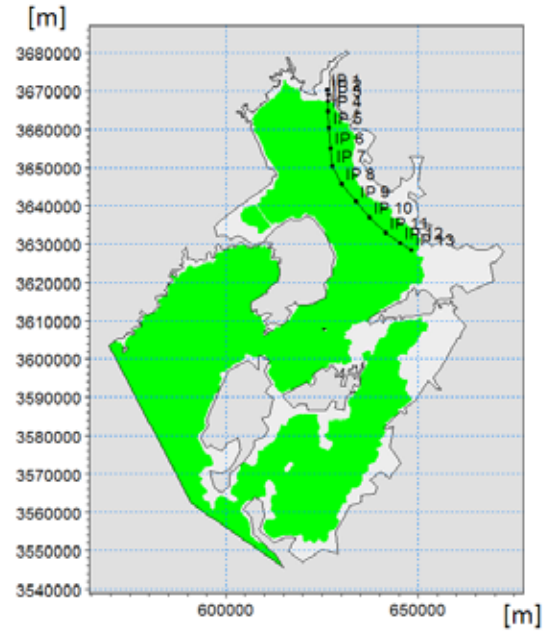

Figure 12.Location of stratification`s points

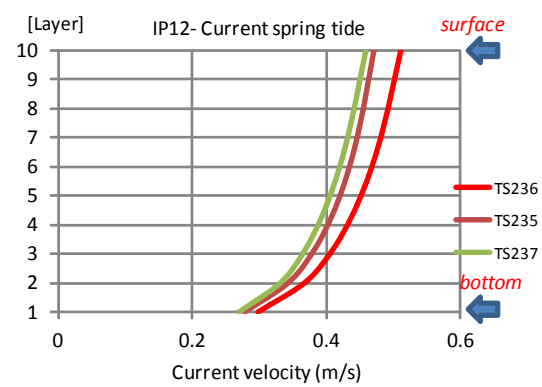

Figure 13.Vertical distribution of Current velocity in IP12 at spring tide

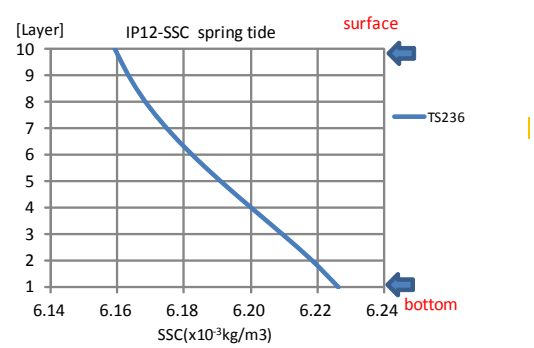

Figure 14. SSC vertical distribution in IP12 at spring

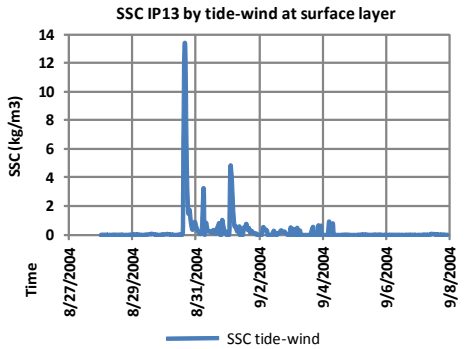

Figure 15. SSC changes by tide-wind concurrent at IP13 in surface layer.

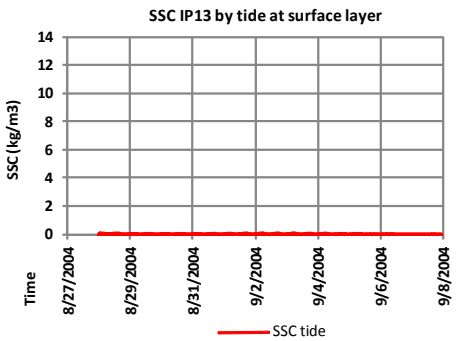

Figure 16. SSC changes by tide concurrent at IP13 in surface layer.

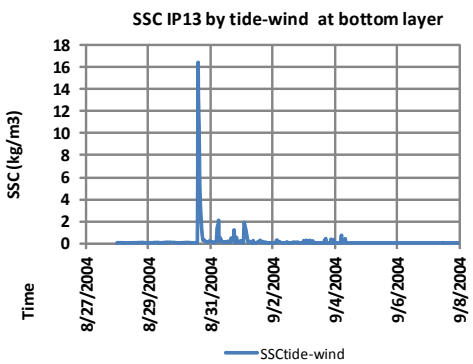

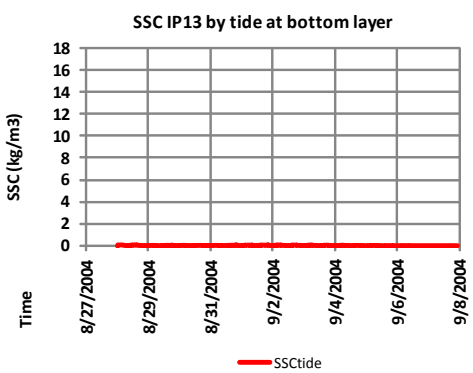

Figure 17. SSC changes by tide versus tide -wind concurrent at IP13 in bottom layer

Table 1. Current velocity of IP1 to IP13 at spring, neap and flooding tide.

IP	Current (m/s)							
	spring				neap			
	surface	direction	bottom	direction	surface	direction	bottom	direction
1	0.4	south	0.2	south	0.065	south	0.03	south
2	0.23	south	0.13	south	0.82	south	0.4	south
3	0.55	south	0.1	north	1.5	south	0.6	south
4	0.55	north	0.2	north	0.7	south	0.1	south
5	0.45	north	0.2	north	0.53	south	0.16	south
6	0.65	north	0.3	north	0.63	south	0.3	south
7	0.85	north	0.5	north	0.8	south	0.4	south
8	0.83	north	0.5	north	0.8	south	0.45	south
9	0.58	north	0.32	north	0.55	south	0.3	south
10	0.55	north	0.32	north	0.53	south	0.32	south
11	0.45	north	0.26	north	0.45	south	0.26	south
12	0.51	north	0.3	north	0.4	south	0.25	south
13	0.35	north	0.175	north	0.56	south	0.3	south

IP	Current (m/s)			
	flooding			
	surface	direction	bottom	direction
1	1.5	south	0.8	south
2	1.6	south	0.8	south
3	1.5	south	0.7	south
4	0.26	south	0.1	north
5	0.48	south	0.17	north
6	-	-	-	-
7	-	-	-	-
8	-	-	-	-
9	-	-	-	-
10	-	-	-	-
11	-	-	-	-
12	-	-	-	-
13	-	-	-	-

Table 2. SSC of IP1 to IP13 at spring, neap and flooding tide.

IP	SSC (kg/m3)					
	spring		neap		flooding	
	surface	bottom	surface	bottom	surface	bottom
1	0.473	0.472	0.442	0.442	0.644	0.663
2	0.450	0.449	0.448	0.458	0.718	0.736
3	0.275	0.100	0.593	0.610	0.880	0.895
4	0.033	0.034	0.470	0.340	0.380	0.180
5	0.022	0.022	0.045	0.032	0.070	0.080
6	0.023	0.023	0.027	0.028	-	-
7	0.030	0.042	0.035	0.036	-	-
8	0.040	0.060	0.050	0.070	-	-
9	0.034	0.035	0.041	0.041	-	-
10	0.022	0.023	0.021	0.019	-	-
11	0.009	0.010	0.008	0.008	-	-
12	0.006	0.006	0.005	0.006	-	-
13	0.005	0.005	0.009	0.009	-	-

V. CONCLUSIONS

SSC and salinity changes due to storm surge and tidal current in the North Ariake Sea have been presented. Based on the simulation result and discussion above, the followings can be concluded.

1). The model has been calibrated against water level, salinity and sediment concentration data, as the good a g r e e - ment.
2). The effect of tidal current deposition took place more to the north and almost along nearshore and river mouth, while erosion at more south.
3). The highest SSC took place near the river mouth caused

by flooding towards the south.

4). Salinity and SSC in vertically and plan view distribution reflect the actual natural phenomena in the Ariake Sea.
5). Wind effected the erosion taking place at almost the all points in basin.
6). The tidal current is on important effect that should be counted to sediment resuspension, while storm surge influenced the most to suspended sediment at strong wind period.
7). urther observation of bed level change of bathymetry and the longer time of simulation in order to evaluate the such steady result condition of salinity and SSC also recommended.

ACKNOWLEDGEMENT

The authors would like to thank all involved directly and indirectly for the completion of this paper. Special thanks to Sam Ratulangi University and Indonesia Government for supporting the study.

REFERENCE

[1]. Ariestides, K.,T.,Dundu., Koichiro Ohgushi. (2012). A Study On Impact Of Storm Surge by Typhoon in Saga Lowland and Surroundings using Hydrodynamic Numerical Modelling. International Journal of Civil & Environmental Engineering,Vol.12 No :01. | [2]. Cao Don, N., et al. (2007). Sediment Transport And Short Term Sediment Process in Tidal Flats Of Ariake Sea. Journal Coastal Research 2007. | [3]. DHI. (2009). MIKE21 and MIKE3 FLOW MODEL FM, Hydrodynamic Module, Step -by- step training guide. | [4]. DHI. (2011). MIKE21 and MIKE3 FLOW MODEL FM, Hydrodynamic and Transport Module, Scientific Documentation. | [5] DHI. (2011). MIKE21 and MIKE3 FLOW MODEL FM, Hydrodynamic Module, User Guide. | [6]. M.,H.,Garcia.(Ed).(2008).Sedimentation Engineering: processes, management, modeling, and practice. Virginia, ASCE | [7]. Saeed Sarbaty. (2012). 3-D Simulation of Wind-Induced Currents Using MIKE 3 HS Model in the Caspian Sea. Canadian Journal on Computing in Mathematics, Natural Sciences, Engineering and Medicine, Vol.3 No.3, March 2012. | [8]. W.,H., McAnally & A.,J., Mehta. (Eds). (2003). Coastal and Estuarine Fine Sediment Processes. Proceeding in Marine Science. Amsterdam, Elsevier. | [9]. Y.,Sonoda, et al. (2011). Distribution Characteristic Of Water Quality Sediment And Benthos In Ariake Sea. Journal JSCE 2011.